EXAMINATION OF DEBRIS CLOUD DENSITY RESULTING FROM PRECESSION OF ARGUMENT OF PERIGEE DUE TO J2 EFFECT

Joel D. Slotten[(1)]

[(1)] *SAIC, 14672 Lee Rd, Chantilly, VA 20151, U.S.A., Email: joel.slotten@SAIC.com*

ABSTRACT

Following an on-orbit breakup event the resulting toroidal debris cloud quickly disperses as the orbital planes of the debris fragments separate due to the J_2 effect. However, the orbital planes will continue to be nearly coincident at their maximum northern and southern declination, resulting in a much higher spatial density of debris at these two locations. Further, the spatial density will increase as the breakup "pinch point" recesses toward one of these nodes, also due to the J_2 effect. Concepts that create "artificial atmospheric drag" using dust particles, liquid vapours, or gas filled balloons could be employed at this location to quickly remove the debris. This technique would be particularly effective if timed to coincide with the arrival of the pinch point.

1 BACKGROUND

Several concepts have been proposed for reducing the orbital lifetime of small debris that involve creating "artificial atmospheric drag." These concepts suggest launching dust particles, frozen liquid, or high density gas into ballistic trajectories or short lived orbits to interact with debris objects in a manner similar to the Earth's atmosphere, thereby decreasing their orbital velocity and decreasing their orbital life [1-5].

However, these concepts are expected to be somewhat inefficient. This is due to the relatively low spatial density of the debris, which results in very few interactions between the debris and the artificial atmosphere. Some have suggested that these methods could be more effective in response to an on-orbit breakup event [1-2]. Initially all fragments from a breakup will pass through a "pinch point" during their orbit as shown in Fig. 1. This is the location in inertial space where the mishap occurred. The high spatial density at this location would make these debris removal methods much more efficient. Unfortunately, perturbations cause this pinch point to quickly dissipate. The J_2 effect in particular causes the right ascension of ascending node (RAAN) of the fragments to precess at different rates due to the variations in their inclinations, semi-major axes, and eccentricities. Therefore, the orbital planes of the fragments spread, and the pinch point disperses over hundreds of kilometres in a matter of days.

The fanning out of the orbital planes is most dramatic at the equator. Nearer the poles, the orbits remain nearly coincident. For this reason, the spatial density of the debris remains fairly constant at these two locations. Once the pinch point expands significantly, it is at the extreme latitudes that the debris cloud is most concentrated.

In addition to its effect on an orbit's RAAN, the J_2 effect also causes the argument of perigee to precess. As a result the pinch point, where the debris are at nearly the same altitude, will drift either to the north or south, contracting as it travels. After several weeks to a few months (depending on the parent object's original orbit and the location of the collision or explosion) the pinch point will reach a maximum density at the orbit's extreme northern or southern declination. This delay in the re-coalescing of the pinch point will allow sufficient time to launch a response if pre-positioned assets are available.

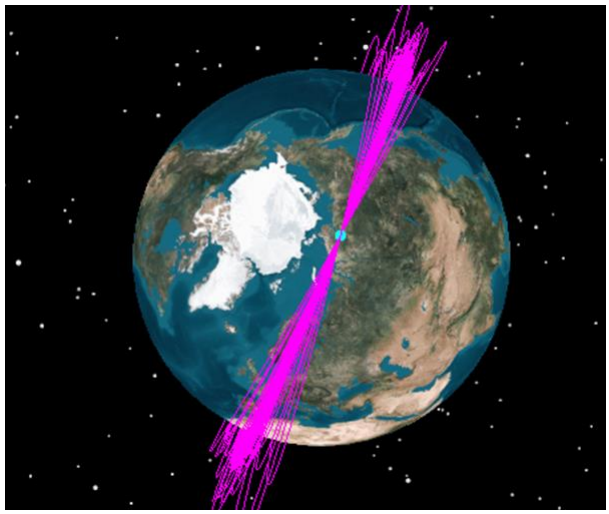

Figure 1. Pinch Point

Using NASA's standard breakup model [6] and an SGP4 propagator [7], this paper demonstrates that for three satellites involved in two major breakup events a majority of fragments passed within approximately 250 kilometres of their pinch points three to four months after the breakup. This could have provided sufficient debris spatial density for an artificial atmospheric drag concept or other debris remediation method to be effective. It also provided sufficient time for a pre-positioned response effort to be launched, had one been available.

Proc. 7th European Conference on Space Debris, Darmstadt, Germany, 18–21 April 2017, published by the ESA Space Debris Office
Ed. T. Flohrer & F. Schmitz, (http://spacedebris2017.sdo.esoc.esa.int, June 2017)

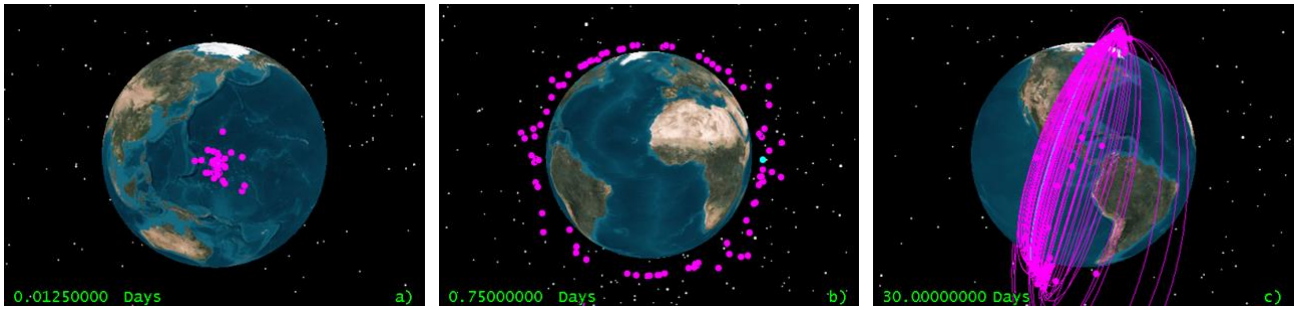

Figure 2. First Three Phases of a Debris Cloud

2 DEBRIS CLOUD EVOLUTION AND DENSITY

Following an on-orbit breakup event a debris cloud will form and evolve through a series of four stages as described by Jehn [8]. Initially the cloud forms an ellipsoid as shown in Fig. 2a. This ellipsoid will elongate almost immediately as the mean anomalies of the debris fragments disperse. Debris thrown into orbits with smaller semi-major axes will lead the cloud while those with larger semi-major axes will trail behind. Within a few hours the cloud will elongate into a toroid as seen in Fig. 2b; the second state of its evolution. This toroid will have a pinch point at the site of the collision or explosion through which all of the debris passes. The maximum radial extent of the toroid will be located 180 degrees out from the pinch point, due to the in-track component of the delta-V experienced by the debris during the breakup event. The maximum out-of-plane extent is at 90 and 270 degrees from the pinch point, due to variation in the debris RAAN and inclination caused by the out of plane component of the delta-V. The density of the debris cloud will be greatest at the pinch point.

During the third phase, the toroid will open and expand as shown in Fig. 2c. This is a result of the perturbations caused by the Earth's uneven gravitational field. The largest component of this perturbation is the second zonal harmonic, or J_2 [9]. The J_2 effect causes both the RAAN and the argument of perigee of an object's orbit to precess. The rate of precession varies based on semi-major axis, inclination, and eccentricity of the orbit. Because the orbital elements of the debris vary somewhat, their RAANs precess at different rates, and the toroid fans out. In addition, the pinch point will rotate toward the north or south due to the precession of the argument of perigee.

The rate of change of RAAN can be expressed as:

$$\dot{\Omega} = -\frac{3nR_E^2 J_2}{2p^2}\cos(i) \qquad (1)$$

And the rate of change of the argument of perigee is:

$$\dot{\omega} = \frac{3nR_E^2 J_2}{4p^2}\{4 - 5\sin^2 i\} \qquad (2)$$

Here n is the mean motion, R_E is Earth's radius, J_2 equals 0.001 082 63, i is inclination and p is the semi-latus rectum.

$$p = a(1 - e^2) \qquad (3)$$

Where a is the semi-major axis and e is eccentricity. Fig. 3 and Fig. 4 show the daily change in RAAN and argument of perigee respectively for circular orbits at various altitudes in kilometres.

During the third phase, the debris density at the pinch point will decrease as the orbital planes separate. Yet this is not the case near the extreme declinations (latitudes). This is because the changes in RAAN have a lesser effect at these locations. As the RAAN changes and the orbital planes fan out, the planes pivot at the maximum declination creating a common node there. At the extreme northern and southern extents of the orbit the argument of latitude (u), defined as the angle between the ascending node and the radius vector of the object, equals 90 and 270 deg. respectively [10]. Fig. 5 shows the northern node 30 days after a breakup.

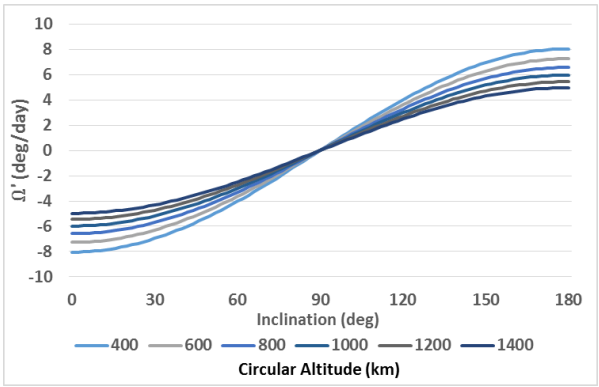

Figure 3. Daily Change in RAAN Due to J_2 Effect

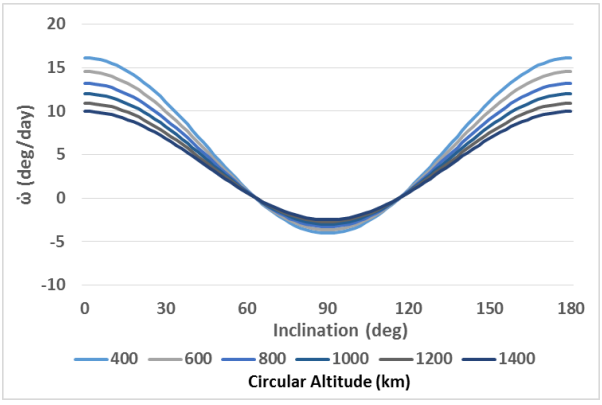

Figure 4. Daily Change in Argument of Perigee Due to J_2 Effect

As the orbital planes fan out, the altitude of the debris as they pass through the pinch point will remain nearly equal, although some variation will develop as the arguments of perigee precess at different rates. As the pinch point precesses it will eventually arrive at the northern or southern node, where the orbital planes of the debris align. At this point, the debris cloud density will increase because both the altitude of the debris (from the pinch point) and the orbital planes (from the node) will nearly align. It is this fact that will be examined in detail in this paper.

The final phase of the debris cloud is an evenly distributed band around the Earth with maximum northern and southern declinations nearly equal to the inclination of the breakup event parent object. Although the cloud will form a complete band once the debris with the fastest nodal precession have caught up to those with the slowest, it will take some time longer, generally years, before the debris is evenly distributed over right ascension [8,11].

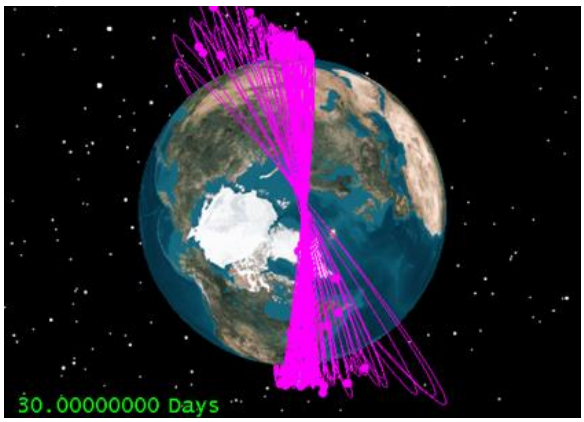

Figure 5. Northern Node (u = 90)

3 DEBRIS OBJECT CREATION AND PROPAGATION

To better understand how the debris density varies during the early portion of the third phase, both at the pinch point and at the northern and southern nodes, a program was written in MATLAB that first models the debris resulting from an on-orbit breakup event and then propagates both the parent object and the debris fragments for a specified time. The model then determines the minimum distance between each object's propagated orbit and the three points of interest: the pinch point, the northern node and the southern node.

To generate the debris NASA's standard breakup model for collisions was used [6]. The number of objects of a given size and larger was determined by using Eq. 4.

$$N(L_c) = 0.1(M)^{0.75} L_c^{-.71} \qquad (4)$$

Lc is the characteristic length in meters and M is the combined mass in kilograms of the colliding objects. Area-to-mass ratio, mass, cross-sectional area, and delta-V for each object were also calculated using equations from [6].

Other authors have focused on developing analytical models of debris cloud evolution, primarily for collision risk assessments. Due to the complex nature of the early phases of cloud evolution some have focused on phase four or late phase three evolution [12,13]. Others have developed models useful for early phase three, but have focused on the gross characteristics of the cloud as a whole [14,15]. For this paper a numerical analysis was performed of the debris clouds' evolution using an SGP4 propagator [7]. This propagator accounts for third body effects, perturbations due to Earth's oblateness (including J_2), atmospheric drag and other relevant effects.

Once the objects were propagated to the desired time each object was propagated for one additional revolution. During this revolution the minimum miss distance between the object and the points of interest (the propagated pinch point and the northern and southern node) was determined.

4 CASE STUDIES

The model as described in section 3 was run using three different satellites as the input. The satellites chosen were the three worst contributors to the current debris population: Fengyun 1C, COSMOS 2251, and Iridium 33. On January 11, 2007, the Chinese destroyed one of their own defunct weather satellites, Fengyun 1C, during a test of an anti-satellite weapon [16]. Two years later, on February 10, 2009, two satellites, Iridium 33 and Cosmos 2251, collided over northern Siberia [17]. As of January 2013 there were 3378 catalogued objects from the Fengyun 1C, 598 from Iridium 33, and 1603 from Cosmos 2251 [18].

The breakups of each of these three satellites were simulated using the model described in section 3. Table 1 shows the number of debris objects generated by the

model for each of the three satellites. Although the number of fragments 10 cm and larger generated by the model falls short of the number of objects catalogued, particularly for the Fengyun 1C, this does not affect the results of this analysis because the evolution of the debris cloud, propagation of the fragments, and relative cloud density by location are what's of interest here, not the number of objects involved.

Table 1. Number of Debris Modelled for Each Satellite

	> 1 cm	> 10 cm
Fenyun 1C	43,747	849
Cosmos 2251	37,949	719
Iridium 33	28,704	568

Fig. 6 shows the delta-V generated by the model for the debris objects from Iridium 33. Fig. 7 is a Gabbard plot showing the altitude of the apogee and perigee for each Iridium debris fragment created by the model as well as the orbital period. As can be seen, approximately one third of the objects (those with perigees below 0 km altitude) immediately de-orbited after the collision. These consisted primarily of objects with the smallest characteristic lengths.

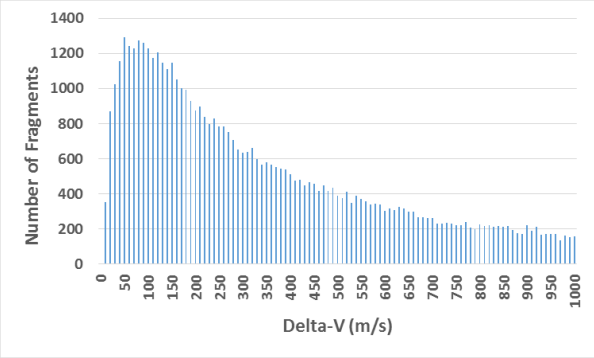

Figure 6. Delta-V from Iridium 33 Breakup

Each breakup was propagated for a certain number of days post-breakup. At each time interval the minimum distance, or miss distance, between each object's orbit and each of three specific locations was determined: the propagated pinch point, the northern node (u = 90), and the southern node (u = 270). The median miss distance values were then plotted. These values represent the radius of the debris cloud at that time and location consisting of half the debris fragments. So if a debris removal technique were effective out to this range it would have been capable of clearing 50% of the debris from the breakup at that location at that time.

Fig. 8 - Fig. 10 show the median miss distances at each location for the three breakup events. As can be seen, the debris clouds are initially densest at the pinch point.

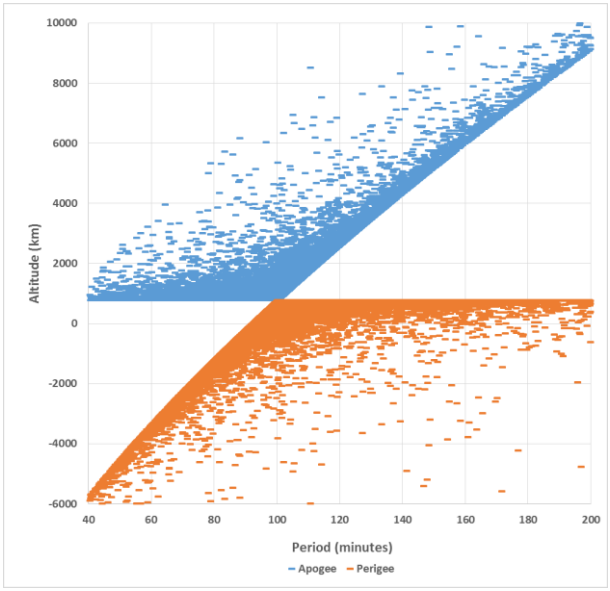

Figure 7. Gabbard Plot of Modelled Iridium Debris

However, the size of the cloud at the pinch point grows over time as the orbit planes separate in RAAN. Eventually, the pinch point contracts again as the argument of perigee precesses and the pinch point approaches one of the declination extrema. Beyond the first few days after the breakup, this was the time that an attempt to remove the debris would have been most effective.

The Iridium-Cosmos collision occurred near the northern node of both satellites' orbit. Initially the pinch point was the location where the debris cloud was the most compact. Yet, within a few days the pinch point expanded enough that the northern node becomes the most compact location. With an inclination of 74.0 deg. for Cosmos 2251 and 86.4 deg. for Iridium 33 the argument of perigee for both debris clouds recessed rather than precessing as can be seen from Fig. 4.

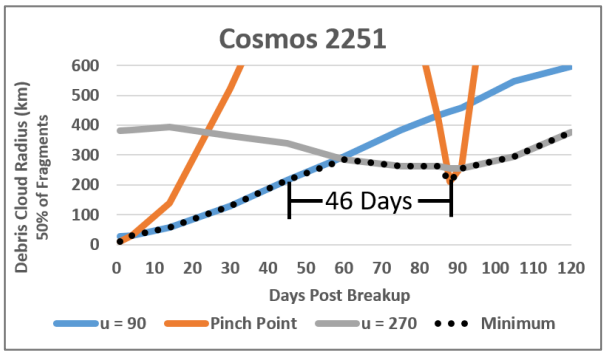

Figure 8-. Required Effective Distance to Remove 50% of Debris – Cosmos 2251

Cosmos had an argument of latitude of 97.2 deg. at the time of the collision, and so the pinch point passed through the northern node within the first four days after the collision. As seen in Fig. 8, the pinch point then

travelled south, and expanded as it did. The cloud at the northern node expanded as well as the pinch point departed, but more slowly. Therefore, at this point in time the northern node was the most compact location within the debris cloud. Meanwhile the cloud was contracting at the southern node, because the altitudes of

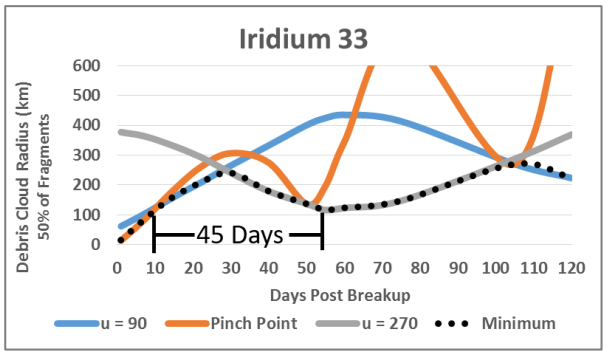

Figure 9. Required Effective Distance to Remove 50% of Debris – Iridium 33

the fragments at that location were converging. Approximately 60 days after the collision the southern node became more compact than the northern node. At the same time, the size of the pinch point reached its local maximum shortly after it crossed the equator and then started to contract as it approached the southern node. The pinch point arrived at the southern node 88 days after the collision. At this point the size of the debris cloud at the pinch point/southern node was at its local minimum, and the cloud was more compact than it had been during the previous 46 days.

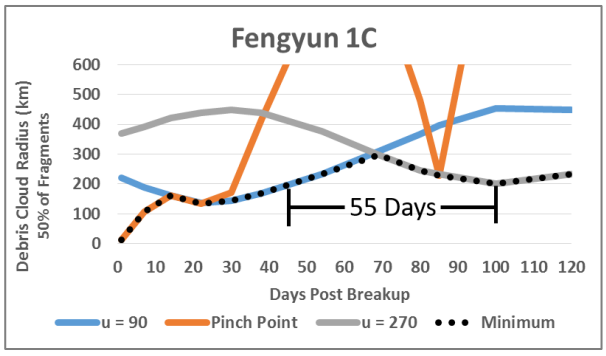

Figure 10. Required Effective Distance to Remove 50% of Debris –Fengyun 1C

A very similar scenario unfolded for Iridium 33. The satellite had an argument of latitude of 72.8 deg. So unlike Cosmos, Iridium's pinch point moved south without passing through the northern node. Even so, the pinch point reached its maximum expanse approximately 28 days after the collision, just as the southern node became the densest location within the debris cloud. The location of the debris fragment miss distances at this time is shown in Fig. 11. Here the greatest extent of the cloud was in the cross-track direction due to the differences in orbital planes. The pinch point arrived at the southern node 50 days after the collision, obtaining its local minimum size when it did. The location of debris miss distances at this time is shown in Fig.12. At this point the greatest extent of the cloud was in the radial direction due to difference in the altitudes of the debris. The distribution of the miss distances at this point are shown in Fig.13. Shortly after the arrival of the pinch point the southern node also reached its local minimum. At this point the cloud was more compact than it had been during the previous 45 days.

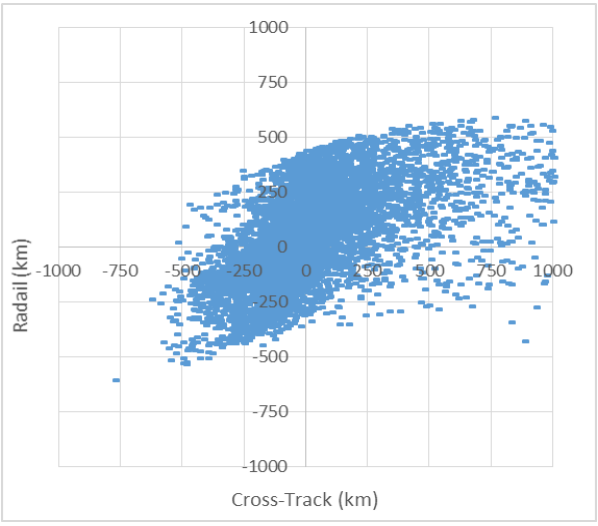

Figure 11. Iridium 33 Pinch Point Miss Distances - Day 28

Comparing Figure 8 and Fig.9 shows Cosmos' pinch point reached the southern node much later than Iridium's. This is not only because Cosmos travelled 24 degrees farther, having traversed the northern node first, but also because its pinch point recessed at a slower rate. Fig. 4 shows that Cosmos' lower inclination resulted in a *slower* rate of change (2.1 deg./day vs. 3.3 deg./day for Iridium).

Cosmos' lower inclination also resulted in a *faster* rate of change for its RAAN compared to Iridium. Not only that, but Fig. 3 shows that at 86.4 deg. inclination, Iridium's RAAN rate of change varies only slightly for different semi-major axes. As a result, the orbital planes did not fan out as quickly. This was manifested in the much lower 307 km size for Iridium's pinch point on day 30 as shown in Fig. 9 compared to Cosmos' 522 km on that same day as seen in Fig. 8. These results are consistent with the ways in which these debris clouds actually evolved after the collision [11].

Fig. 4 shows that with an inclination of 98.6 deg. Fengyun 1C had the same rate of change for the argument of perigee as a satellite with an 81.4 deg. inclination. Therefore, Fengyun's argument of perigee changed at a rate between that of Iridium and Cosmos. Likewise, Fig. 3 shows Fengyun's RAAN rate of change was also between that of Iridium and Cosmos, but in the opposite direction because Fengyun's orbit was retrograde.

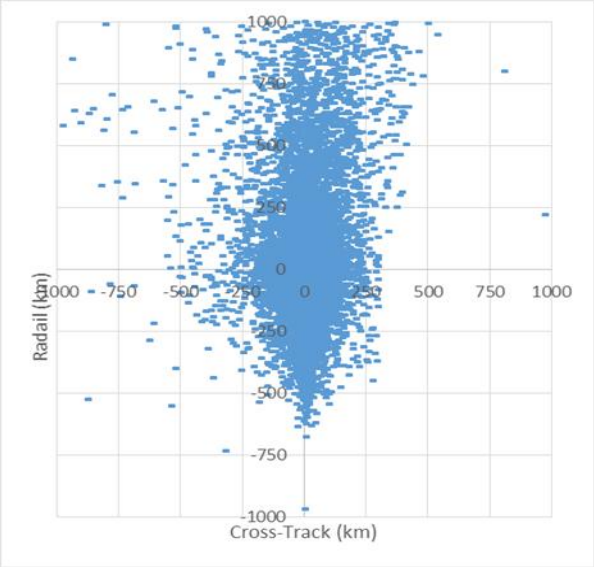

Figure 12. Iridium 33 Pinch Point Miss Distances - Day 50

Fengyun 1C's initial argument of latitude of 152 deg. and negative change in argument of perigee meant the pinch point initially moved toward the northern node, reaching it 22 days after the breakup. Afterward the pinch point rapidly expanded, and the northern node became the most compact location within the debris cloud. However, as with the other two breakups, the northern node also started expanding at this point, although at a slower rate than the pinch point. After 69 days the southern node became the most compact location within the cloud. The southern node continued to contract until day 100, 15 days after the pinch point arrived. At this point the cloud was more compact than it had been during the previous 55 days.

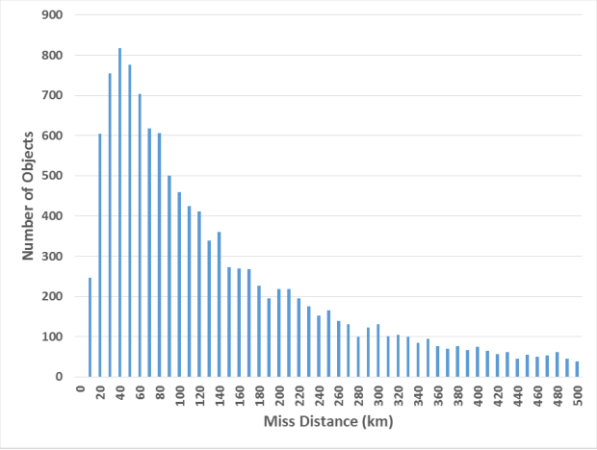

Figure 13. Distribution of Iridium 33 Pinch Point Miss Distances - Day 50

These results demonstrate how waiting might be an effective strategy for removing debris following a breakup event. An immediate response at the pinch point would have been most effective if a debris removal system had been available. However, for all three breakup events the northern node became denser than the pinch point within a few days (4 days for Cosmos, 11 for Iridium, and 22 for Fengyun). The northern node therefore became the better location for a response effort. Eventually, the northern node expanded so much that it would have made more sense to wait for the pinch point to arrive at the southern node where $u = 270$. This would have resulted in a denser cloud and more debris fragments removed. This cross-over point, where waiting would have been the best strategy, occurred at 42 days post-breakup for Cosmos, 10 days post-breakup for Iridium, and 45 days post-breakup for Fengyun.

Although these results seem promising for these three satellites, this technique will not work for all breakup events. The arguments of perigee of satellites near the critical inclinations of 63.4 deg. or 116.6 deg. will precess extremely slowly as can be seen from Fig. 4. As a result the pinch point may take so long to reach one of the nodes that the debris cloud is no longer compact once it arrives.

5 CONCLUSIONS

Removal of orbital debris fragments from the environment surrounding Earth is a particularly challenging endeavour in part due to the relatively low spatial density of those fragments. Attempts to remove the debris would be much more successful if they took place shortly after the breakup event that originally generated the fragments, before the debris disperses into the background population. Targeting the correct location during the weeks after the breakup would further increase the efficiency of any clean-up effort. Although the spatial density of fragments at a debris cloud's pinch point will quickly decrease, the density at the cloud's northern and southern nodes will remain relatively high, peaking with the arrival of the pinch point, which precesses due to the J_2 effect. If the response effort can be launched at one of the two nodes, and timed with the arrival of the pinch point, the greatest amount of debris can be removed.

6 REFERENCES

1. Ganguli, G. et al. (2011). A Concept for Elimination of Small Orbital Debris. arXiv:1104.1401.
2. Gregory, D. et al. (2012). Space Debris Elimination (SpaDE) Phase I Final Report. NASA NIAC—11-NIAC-0241.
3. Dunn, M. Space Debris Removal (2012). *United States Patent Application Publication*, Pub. No. US 2012/0241562 A1.
4. Phipps, C. R. et al. Removing Orbital Debris with Lasers. arXiv: 1110.3835.

5. Pelton, J. (2013). *Space Debris and Other Threats from Outer Space*, Springer Science & Business Media, New York, p. 34.

6. Johnson, N. L. et al. (2001). NASA's New Breakup Model of EVOLVE 4.0. *Advances in Space Research*, **28**(9), 1377-1384.

7. Rino, C (2010). Satellite Orbit Computation Online at *https://www.mathworks.com/matlabcentral/fileexchange/28888-satellite-orbit-computation/content/SGP4/sgp4.m*

8. Jehn, R. (1990). Dispersion of Debris Clouds from On-Orbit Fragmentation Events. *IAA-90-565, 41st Congress of the International Astronautical Federation*, Dresden, GDR.

9. Vallado, D. A. (2013). *Fundamentals of Astrodynamics and Applications*, Microcosm Press, Hawthorne CA, pp 647-665.

10. Bates, R. R. et al. (1971) *Fundamentals of Astrodynamics*, Dover Publications, Inc., New York, p. 60.

11. Pardini, C, et al. (2011). Physical Properties and Long-Term Evolution of three Debris Clouds Produced by Two Catastrophic Collisions in Earth Orbit. *Advances in Space Research*. doi: 10.1016/j.asr.2011.04.006.

12. Barrows, S. (1996). Evolution of Artificial Space Debris Clouds. *University of Southampton, Engineering and Applied Science, Department of Aeronautics and Astronautics*, PhD Thesis.

13. Frazzoli, E., et al. (1996). Debris Cloud Evolution: Mathematical Modelling and Application to Satellite Constellation Design. *Acta Astronautica*, **39**(6),439-455.

14. Letizia, F., et al. (2015). Multidimensional Extension of the Continuity Equation Method for Debris Clouds Evolution. *Advances in Space Research*. http://dx.doi.org/10.1016/j.asr.2015.11.035.

15. Letizia, F. (2016). Space Debris Cloud Evolution in Low Earth Orbit. *University of Southampton, Engineering and the Environment, Department of Aeronautics, Astronautic and Computational engineering*, PhD Thesis.

16. NASA Orbital Debris Program Office (2007). Chinese Anti-Satellite Test Creates Most Severe Orbital Debris Cloud in History. In *Orbital Debris Quarterly News*, **11**(2).

17. Kelso, T. S., Analysis of the Iridium 33-Cosmos 2251 collision (2009). *Advances in the Astronautical Sciences*, **135**(2), AAS 09-368, 1099-1112.

18. NASA Orbital Debris Program Office (2013). An Update of the FY 1C, Iridium 33, and Cosmos 2251 Fragments. In *Orbital Debris Quarterly News*, **17(**1), 4-5.